[1]Hansi Fu*

Artistic Creation and Animation Scene Designing using Hierarchical Spatio-Temporal Graph Convolutional Neural Network Optimized with Gazelle Optimization Algorithm

JES Journal of Electrical Systems

Abstract: - Creating moving visuals, usually in the form of 2D or 3D animations, is the focus of the graphic design field known as animation design. A sequence of consecutive images, or frames, is played quickly one after the other in animation design to provide the impression of motion. In this Manuscript, Artistic Creation and Animation Scene Designing using Hierarchical Spatio-temporal graph convolutional neural network Optimized with Gazelle Optimization (AC-ASD-HSTCNN-GO)is proposed. Initially, data is taken from LiDAR dataset then the data are fed to preprocessing segment. For pre-processing Orthogonal Master Slave Adaptive Notch Filter (OMSANF) is used to remove duplicate data and replacing missing data from collected data's. Then the feature are extracted by using General Synchroextracting Chirplet Transform (GSCT) technique, which extracts features such as objects, faces and scenes. Finally HSTGCNN for creating 3D animation image design .In general the HSTGCNN does not express some adaption of optimization strategies for determining optimum parameters to assure the product recommendation. Hence, the GOA is proposed to enhance HSTGCNN.The proposed AC-ASD-HSTCNN-GO method is activated in python and the performance of proposed AC-ASD-HSTCNN-GO is estimated under performance metrics like accuracy, precision, F1-score, recall, specificity, computational time, error rate, RoC. Finally, performance of AC-ASD-HSTCNN-GO method provides 15.27%, 17.14%, 18.58% greater accuracy, 16.11%, 19.65%, 20.53% greater precision and 19.31%, 21.29%, 22.15% greater F1-Score while compared with existing techniques like Graphic Design of 3D Animation Scenes Depend on Deep Learning with Information Security Technology (GD-3DASDL-IST), GRADE: Generating Realistic Animated Dynamic Environments for Robotics Research (GRADE-RR)andApplication of Random Forest Algorithm in Natural Landscape Animation Design (ALN-RFA-NLAD) respectively.

Keywords: Gazelle Optimization Algorithm, General Synchroextracting Chirplet Transform, Hierarchical Spatio-temporal graph convolutional neural network, Orthogonal Master Slave Adaptive Notch Filter.

I. INTRODUCTION

In recent years, there has been a lot of research, attention attentive on three-dimensional (3D) animation scene design as an important part of digital entertainment, gaming, and advertising. There are still numerous obstacles to overcome in the quest for effective and superior design processes. Integrating information security and deep learning (DL) technologies has come to be as a critical path for accomplishing inventive advancement in order to address these issues [1-3]. DL technology's strong feature extraction and pattern recognition skills have led to its enormous success in a variety of sectors. The CNNs, GANs are two examples of deep learning models that have shown exceptional picture production and transformation capabilities, particularly in image processing. This creates fresh opportunities for scene creation in 3D animation [4-6]. With the use of DL models, a scene's characteristics and details may be inferred from a huge amount of data, producing photographs that are more inventive, realistic, and of excellent quality. Nevertheless, even with the great potential of DL technology, there are still a lot of issues that need to be resolved for its implementation in 3D animation scene design, such as data security, image quality, and training stability [7-9]. In the meanwhile, it is impossible to overlook the significance of information security technologies in the world of technology. Protecting intelligent property rights, image data security is essential, particularly in the realm of digital entertainment. It is essential to concentrate on picture development while designing 3D animation sequences and to think about safeguarding these images against the risk of malicious theft, alteration, and damage [10-12]. Thus, IST integration in 3D animation graphic design enhance generated image security while also offering more dependable assurances to the digital entertainment sector. In order to do in-depth investigation, analysis on graphic design in 3D animation scenes, application of DL processes to animation graphic design was explored through use of computer-aided virtual reality [13-15]. The research considered all frame of3D animated character image as scene from a digital sculpture, discovered the use of 3D animation provided solutions for issues such as the weighting of digital sculpture software, suggested a method for designing animation for films and television utilizing 3D visual communication technology, utilized DL to extract depth features [16].

[1*] Lecturer, Information and Art Design Department, Henan Forestry Vocational College, Luoyang, Henan, 471002, China
*Corresponding author e-mail: juliette4030@163.com

Based on visual communication, the animated video images and multi-frame animation were recreated [17]. In short amount of time, our investigation may be able to rebuild video pictures with high precision automatically generated lifelike speech animations synced with the input voice using DL techniques [18]. These existing studies, demonstrating how researchers may effortlessly modify the simulation to suit their specific needs, such as object interactions and visual settings, current approaches directly build upon Isaac Sim's work and help to further close the gap among simulation, real-world scenarios [19]. These disadvantages of the existing methods motivate as do this work [20].

Major contribution of this paper includes,

- Artistic Creation and Animation Scene Designing using HSTGCNN Optimized with GOA is proposed.
- It gathers color images of 3D animated scenes from different points of view. Using a HSTGCNN, this piece provides high-quality point network results and visualizes data in three dimensions.
- Lastly, an analysis is conducted on the efficiency of the enhanced HSTGCNN for developing 3D animation scene graphics and the impact of various enhanced models to the generation of 3D animation scene images.
- The created 3D animation scene continuously improves in image quality, and the fluctuation in generator loss is reduced.
- The developed 3D animation scene's image quality continuously improves, and the generator loss variance is reduced.

Rest of this paper is organized as below: part 2 presents literature review, part 3 designates proposed method, part 4 demonstrates outcome with discussion, part 5 conclusion.

II. LITERATURE REVIEW

Amongst numerous investigation works are DL depend Animation Scene Design using deep learning most numerous current investigation works were reviewed here.

Tang et al. [21] have presented GD of 3DASDL and IST. It creates high-quality point cloud visualizations and enhances the GAN model using the CNN, Earth-Mover distance, Least Squares Method. Lastly, an analysis was conducted on the efficiency of the enhanced GAN in creating 3D animation scene graphics and the contributions of various enhanced models to the generation of 3D animation scene images. It provides higher accuracy but it provides lower precision.

Bonetto et al. [22] have presented generating realistic animated dynamic environments for robotics investigation. They overcome this by introducing a completely adaptive framework called GRADE, which creates realistic animated dynamic settings for robotics investigation that was mainly concerned with robot vision. The system can be used to experiment with robots online in dynamic situations, or it utilized to provide ground truth data for robotic vision connected tasks, offline processing. They enhance the NVidia Isaac Sim to enable customization of robot control. They offer ways to handle the data, populate and manage the simulation, and add assets. They create video datasets of an interior dynamic environment with GRADE's autonomous robots. Initially, they employ it to showcase the visual realism of the framework by assessing sim-to-real gap using YOLO, Mask R-CNN tests. Secondly, they use this dataset to benchmark dynamic SLAM techniques. This method provides higher precision but it provides lower F1-score.

Zhao and Zhang [23] have presented application of a RFA in NLAD. Based on such idea, natural landscape animation design technique presented has self-learning capability. This method introduces RF, which was used throughout animation design method. In order to direct automatic NLAD and produce user-satisfactory animations, RF create a learning method using user assessment as classification outcome. In addition, RF-based NLAD is self-learning and capable of continuously updating the learning model in response to user requirements. This method provides higher recall but it provides lower specificity.

Shan and Wang [24] have presented animation design depend on 3D visual communication technology. The process of reconstructing multiframe animation, animated video images depend on visual communication involves collection of deep features using DL. It was used to identify and extract frame feature of the video image under grey display, and it also completes animation design depend on 3D visual communication technology. According to experimental outcomes, suggested technology may rapidly and accurately recreate

video images while also greatly improving visual transmission of animated video images. This method provides lower computational time but it provides lower accuracy.

Li et al. [25] have presented Deconstruction of Immersive Animation Image Interaction Design under Virtual Reality Technology. This piece presents the idea of animation art design depend on VR technology after first optimizing animation modelling technology and combining it with art design. It then employs interactive technology and art design in a comprehensive way to create virtual space. This demonstrates how people's emotional swings and psychological barriers can be eased by the inviting and comfortable animation art design. This method provides higher recall but it provides lower precision.

Wu et al [26] have presented Multimedia Character Modeling Design and Modeling of Cartoon Animation Depend on Bayesian Sequence Recommendation Process. It deliberates how cartoon animation for multimedia needs to project positive energy and conform to mainstream ideals. This will enable the provision of relevant decision-making frameworks for the production of animation and related outcomes, as well as relevant reference modes for the manufacturing of cartoon animation multimedia characters. Ultimately, goal was to accelerate the completion of corresponding cartoon animation multimedia characters, enhance the efficiency of cartoon animation multimedia works. This method provides lower recall but it provides lower specificity.

Xu [27] have presented new MG 2D animation design technique under perspective of convergence media utilizing intellectual design technology. In present setting, animation design has expanded beyond creation in two or three dimensions and has given origin to a brand-new genre of animation called MG animation. People's opinions about MG animation have changed due to its flexible rhythm and straightforward visual modelling features. Similar to the present manner of new media communication, MG animation deliver high number of dynamic images, text to people in short amount of time when the information was transmitted via Internet. The MG animation's visual performance can enhance the attractiveness and attraction of content. This method provides high Roc but it provides lower accuracy.

III. PROPOSED METHODOLOGY

Artistic Creation and Animation Scene Designing using HSTCNN Optimized by GOA is proposed. Block diagram of AC-ASD-HSTCNN-GO approach is shown in is shown in Figure1. Data acquisition, Artistic Creation and Animation Scene and optimization of the three processes that make up this method. Consequently, a full explanation of each step is provided below.

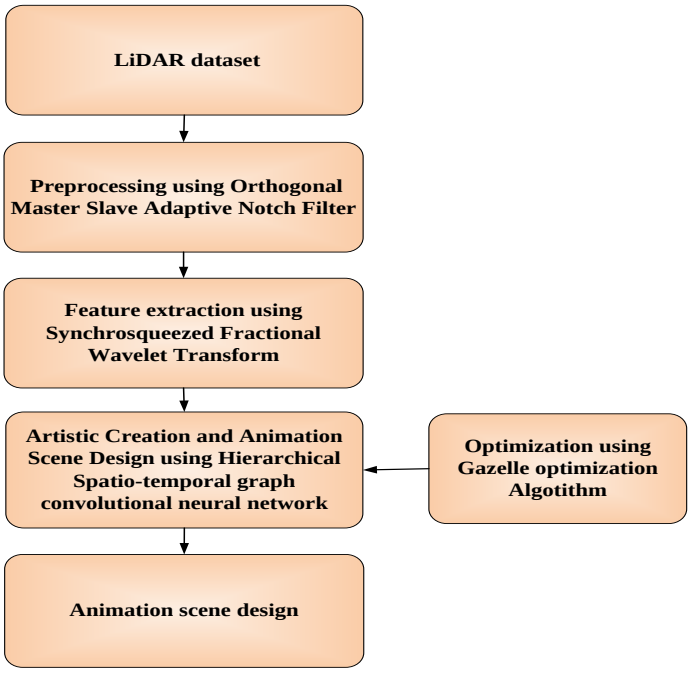

Figure 1: Block diagram of AC-ASD-HSTCNN-GO approach

A. Data Acquisition

The input data gathered from LiDAR dataset [28] it is used to study the Earth's surface. A side and top-down picture of the Loggerhead Key Lighthouse in Dry Tortugas, Florida, is shown using LiDAR data obtained by NOAA survey aircraft. LiDAR data was initially only provided in ASCII format. Due to the enormous

volumes of LiDAR data collected, LAS, a binary format, was quickly adopted to control and standardize the distribution and organization of LiDAR data. Currently, LAS is widely used to represent LiDAR data.

B. preprocessing using Orthogonal Master Slave Adaptive Notch Filter

In this step, OMSAF [29] utilized for reducing size, complexity of the data and removes the content which is no more needed as well as texts related filtering. Image processing, which forms the foundation of computer vision; mostly depend on signal reconstruction under specific conditions. A 3D structural reconstruction is not what this reconstruction is. It mentions to the initial data that replenishes the signal, like noise reduction. It is clear from the description above that frequency adaption is crucial for master slave ANF in order to receive correct tracking data. They may quickly examine how the frequency adaptation's convergence is expressed as given in equation (1)

$$\dot{\hat{\omega}} = -\frac{\gamma}{2\xi} y_i (\ddot{x}_1 + \hat{\omega}^2 y_1) \tag{1}$$

where, ξ is the quicker filter responds and ξ controls the filter's response speed is achieved. $\dot{\hat{\omega}}$ Denotes the study state ω denotes the data covariance y_i denotes the complexity image and y_1 denotes the compact domain. The convergence $\dot{\hat{\omega}}$ of will be rapid when it runs at a high speed and slow when it runs at a low pace. This complicates the adjustment of γ. When close to periodic orbit designated as the given in equation (2)

$$y_1^2 = -\frac{A}{\omega_1}\cos(\omega_1 t + \theta_1) \tag{2}$$

where, A defines the amplifier, ω_1 denotes the frequency and θ_1 describes the initial phase. y_1^2 denotes the spares spectrum and t denotes the translation. To address these issues, a refined frequency adaption method is suggested. Here, the stability of the suggested frequency adaptation is examined. Near the periodic orbit, one possesses the given in equation (3)

$$\dot{\hat{\omega}} = -\frac{\gamma}{2\xi\omega_1}\left[B^2(\hat{\omega} - \omega_1) + B^2(\hat{\omega} - \omega_1)\cos(2(\omega_1 t + \theta_1))\right] \tag{3}$$

here, ω_1 denotes the rotor speed, ξ is the quicker filter responds, ω denotes the frequency and θ_1 describes the initial phase, B defines the amplifier, t denotes translation γ and this complicates the adjustment matrix. Therefore, the convergence of $\dot{\hat{\omega}}$ will be quick when SPMSM operates at a high speed and slow when it operates at a low speed. This complicates the adjustment of γ, additionally the convergence of frequencies is accompanied by the double-frequency oscillation, which impairs frequency estimation performance thus removes the content is given in equation (4)

$$\dot{\hat{\omega}} = -\gamma(\hat{\omega} - \sqrt{\dot{y}_{1\alpha}^2 + y_{1\beta}^2} \Big/ \sqrt{y_{1\alpha}^{\cdot 2} + y_{1\beta}^{\cdot 2}}) \tag{4}$$

where, $y_{1\alpha}^2$ denotes the study state error and $y_{1\beta}^2$ indicate the remove filter. Then reducing size the complexity of the data is shown in equation (5)

$$\varepsilon_\alpha(t) = e_b - \sum_h^n \dot{x}_{h\alpha} \tag{5}$$

This derivation specifies local stability of frequency adaptation able to be ensured. And γ defines convergence rate of frequency, ε_b denotes the double oscillation frequency, n denotes the pure sinusoidal signal and h denotes the specific harmonics $x_{h\alpha}$ is the erroneous data, e_α denotes the spares spectrum and t denotes the translation. Finally, OMSAF filter is prepared the data and information in an appropriate format, these pre-processed data is given into feature extraction phase.

C. Feature Extraction using General Synchro extracting Chirplet Transform

In this section, General Synchro extracting Chirplet Transform (GSCT) [30] discussed to extract the features such as objects, faces and scenes. The DL models that are currently in use have the ability of automatically extracting patterns and features from huge amounts of data to facilitate challenging tasks like image identification. After that, large annotated image data is used to train the model so that it is able to predict new images. The definition for the image is given in equation (6)

$$S_{\alpha,\sigma}(\tau,\omega)=\int_{R} h(t)\psi^{*}_{\alpha,\sigma}(t-\tau)\exp(-j\omega(t-\tau))dt \tag{6}$$

where, $S_{\alpha,\sigma}$ denotes the Chirplet rate, $\psi^{*}_{\alpha,\sigma}$ indicate the complex conjugate, ω is the wavelength, $(\tau \, and \, t)$ is the instantaneous amplitude, j is real part of the image , dt is the optimal image, $h(t)$ denotes analytical image . $\omega_{\sigma}(t)$ denotes Gaussian window function is given in equation (7)

$$\omega_{\sigma}(t)=\frac{1}{\sqrt{2\pi\sigma}}\exp\left(\frac{-t^{2}}{2\sigma^{2}}\right) \tag{7}$$

where, $\omega_{\sigma}(t)$ is denotes the Gaussian window, σ denotes the amplitude and t denotes the time frequency. π signifies processed signal $f(t)\in L^{2}(R)$ as time-varying IF image, its analytic signal $h(t)\in L^{2}(R)$ is given in equation (8)

$$h(t)=A(t)e^{j\phi(t)} \tag{8}$$

where, $h(t)$ denotes amplitude, $j\phi(t)$ denotes the phase of $h(t)$, and $A(t)$ is the window function. The form of the tested image is given in equation(9)

$$\hat{\omega}(t,\omega)=\frac{\partial_{t}S_{\psi}(t,\omega)}{jS_{\psi}(t,\omega)} \tag{9}$$

where, ∂_{t} denotes the initial clearance and ω denotes the radius stiffness. Then extract the features is shown in equation (10)

$$K(TS(t_{0},\omega,\alpha))=\frac{E(TS^{4}(t_{0,}\omega,\alpha))}{E(TS^{2}(t_{0},\omega,\alpha))^{2}}-2 \tag{10}$$

The maximum value of series of kurtosis is designed, parameter value corresponding to maximum value of kurtosis is taken as optimal parameter value at time point t_{0}. Where, t_{0} denotes the modulation operator, E denotes the damping coefficient, K is the processed image, ω is the wavelength, α is the generated distribution data and TS denotes the chirp rate. Finally, GSCT extract the features such as objects, faces and scenes. Afterwards the extracted data is given to HSTGCNN method.

D. Artistic Creation and Animation Scene Design using Hierarchical Spatio-temporal graph convolutional neural network

In this section, Artistic Creation and Animation Scene Designing using HSTGCNN [31]. In order to sum out picture recognition occurs using HSTGNN. It is meant to create data which does not exist, kind of like giving artificial intelligence autonomy to innovate. The discriminator's objective is to distinguish between original and fake photos, assuming that the training set contains actual images. During "conflict," the discriminator uses ongoing recognition to determine the validity of the image as much as possible, while the generator uses ongoing training to produce as many fake images as possible. First, create a collection of spatial graphs, $G(t)$ that symbolize graph structure. The definition of is $G(t)$ given in equation (11)

$$G(t)=(V(G_{t}),\, E(G_{t})) \tag{11}$$

where, V denotes the indices, E indicate the set of coordinate and $G(t)$ denotes the relative position. V g is V^l composed of the coordinates of body joints f and geometric centres p (G_t), in that order. Set of edges in a graph, denoted as $E(G_t)$, can be written is given in equation (12)

$$E(G_t) = \left\{ e_t^{ij} \mid \forall i, j \in \mathrm{N}^* \right\} \tag{12}$$

where, e_t^{ij} represents distance among i^{th} node and j^{th} node N denotesvertices in higher-level graph and lower-level graph. Additionally, input to HSTGCNN incorporates adjacency matrix that shows relative placements of nodes in given in equation (13)

$$a_t^{ij} = \begin{cases} \dfrac{1}{(V_i(G_i) - V_j(G_t))^2}, & (V_i(G_t) - V_j(G_t))^2 \neq 0 \\ 0, & (V_i(G_t) - V_j(G_t))^2 = 0 \end{cases} \tag{13}$$

where, $G(t)$ denotes the relative position, a_t^{ij} weighted adjacency matrix, V_i graph structure and V_j indicate the graph embedding. Normalize the adjacency matrix to help the model converge more smoothly. Frame adjacency matrix A can be written as given in equation(14)

$$A_t = D^{-\frac{1}{2}} \hat{A}_t D^{-\frac{1}{2}} \tag{14}$$

where, D denotes diagonal nodal degree matrix of A_t .Using NN models with images as input, categories as output is a popular way to use deep learning for image recognition. Then developing 3D animation the generation of 3D animation scene images is given in equation (15)

$$H^{(l+1)} = \sigma(D^{-\frac{1}{2}} A D^{-\frac{1}{2}} H^{(l)} W^{(l)}) \tag{15}$$

where, $W^{(l)}$ denotes matrix trainable parameters, l and σ denotes nonlinear activation function. Finally, HSTGCNN to generate the high quality 3D animated scenes. After Gazelle Optimization Algorithm is used to enhance HSTGCNN weight parameter $E\,and\,G_t$ Here, GOA is used to turning the weight and HSTGNN bias parameters.

E. Optimization of HSTGCNN using Gazelle Optimization

In this section, optimization of HSTGCNN using gazelle optimization algorithm (GO) [32] is discussed. The suggested steps for optimization are established, and GOA is offered. The GO is population-depend optimization technique may be applied to any kind of optimization issue. This method develops an optimization algorithm by using the mathematical formulation of the social and hierarchical lives of gazelles. The gazelle must constantly flee from its attackers in order to survive since it knows that if it does not escape and defeat them, it will become dinner for the day.

Step 1: Initialization phase

Setting up the prospective gazelle population as shown in the GO optimization process. Among upper bound, lower bound of given issue, population is formed stochastically. The initialization phase depicted using the equation (16)

$$Y = \begin{bmatrix} y_{1,1} & y_{1,2} & \cdots & y_{1,d-1} & y_{1,d} \\ y_{2,1} & y_{2,2} & \cdots & y_{2,d-1} & y_{2,d} \\ : & : & y_{i,j} & : & : \\ y_{n,1} & y_{n,2} & \cdots & y_{n,d-1} & y_{n,d} \end{bmatrix} \tag{16}$$

where, Y denotes current candidate population, $y_{i,j}$ denotes the position of the i^{th} dimension of j^{th} population, n indicate total number of candidate population, d signifies dimension of problem.

Step 2: Random generation

Input parameters are made randomly. The best fitness values are selected depend on obvious hyper parameter condition.

Step 3: Fitness Function

It creates random solution from initialized values. It is calculated by optimizing parameter. Then the formula is derived in equation (17)

$$Fitness Function = optimizing\ [E and G_t] \tag{17}$$

Step4: Exploration Phase

The instant an attacker is sighted, the exploring phase begins. They replicated this feature by changing the 2m height to a figure among 0, 1. The gazelles' reaction to danger is to kick their feet, flip their tail, or adopt jumping method well-known as "jumping," entails jumping into air up to height of2m with each four feet. For this part of the algorithm, they used the Levy flight, which entails making small steps and sometimes large jumps. The mathematical method of behaviour of gazelle once it spots predator is given in equation (18)

$$\overrightarrow{gazelle_{i+1}} = +R.\mu.\vec{S} * .\overrightarrow{S_L} * .(\overrightarrow{Elite_l} - \overrightarrow{S_L} * .\overrightarrow{gazellei}) \tag{18}$$

where, S denotes top speed, $\overrightarrow{S_L}$ denotes vector of random number, $\overrightarrow{gazelle_{i+1}}$ denotes solution of next iteration $\overrightarrow{gazellei}$ denotes solution of current iteration and μ indicate direction. The mathematical method for behaviour of predator chasing gazelle is given in equation (19)

$$\overrightarrow{gazelle_{i+1}} = \overrightarrow{gazelle_i} + R.\mu.C.F * .\vec{S}_B * .(\overrightarrow{Elite_i} - \overrightarrow{S_L} * .\overrightarrow{gazelle_i}) \tag{19}$$

where, C.F denotes the parameters and $\vec{S}_B$ denotes the random numbers. Figure 2 shows flowchart of GO for optimizing HSTGCNN.

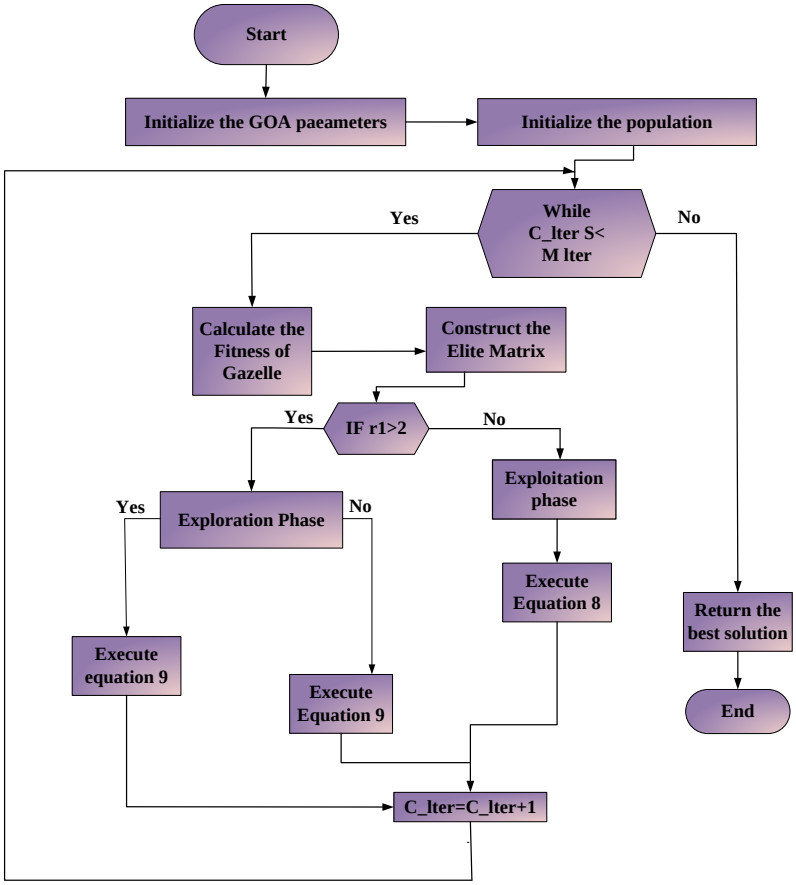

Figure 2: Flowchart of GO for optimizing HSTGCNN

Step5: Exploitation

This stage is predicated on the idea that the gazelles are either happily grazing in absence of a predator or that predator is pursuing gazelles. During this stage, they efficiently covered the domain's surrounding territories using Brownian motion, characterized by uniform with controlled steps, is given in equation (20)

$$\overrightarrow{gazelle_{i+1}} = \overrightarrow{gazelle_l} + r.\vec{S} * .\vec{S}_B * .(\overrightarrow{Elite_l} - \overrightarrow{S_B} * .\overrightarrow{gazelle_i}) \tag{20}$$

where, $\vec{B}_B$ denotes the vector containing random number and s indicates the grazing speed.

Step 6: Termination

The weight parameter values are optimized $E and G_t$ from HSTGCNN is enhanced by using GOA; it will repeat step 3 until it attains halting criteria $Y = Y + 1$ is satisfied. Then HSTGCNN artistic creation and animation scene design effectively.

IV. RESULT AND DISCUSSION

The result of proposed AC-ASD-HSTCNN-GO method is discussed. The proposed AC-ASD-HSTCNN method is simulated in python. The performance of AC-ASD-HSTCNN technique is assessed under some metrics such as accuracy, precision, F1-score, recall, specificity, error rate, computational time and RoC. Obtained results of technique are analysed with existing techniques, likes GD-3DASDL-IST, GRADE-RR and ALN-RFA-NLAD.

A. Performance Measures

A few parameters are utilized to run tests and assess system performance. Performance indicators such as accuracy, precision, F1-score, recall, specificity, error rate, computational time, RoC are studied. Measure performance metrics, confusion matrix is deemed. Measure the confusion matrix likes True Negative, True positive, False Negative, False positive values are needed.

1) Accuracy

It is a metric that measures overall correctness of forecasts made by classification method. It defines ratio of exact forecasts to total instances.

$$Accuracy = \frac{TP + TN}{FN + TP + FP + TN} \tag{21}$$

here, TP denotes true positive, TN denotes true negative, FN represents false negatives, FP represents false positive.

2) Precision

It is a metric that quantifies accuracy of positive forecasts made by classification method. It defines ratio of true positives to sum of true and false positives.

$$\Pr ecision = \frac{TP}{FP + TP} \tag{22}$$

3) F1- Score

It is well-known as F1 score, is metric combines precision and recall to single value. It is mainly valuable in situations where you want to balance both false positive, false negative.

$$F1 - Score = 2 \times \frac{\Pr ecision \times \mathrm{Re}call}{\Pr ecision + \mathrm{Re}call} \tag{23}$$

here, precision represents ratio of true positive to sum of true and false positive.

4) Recall

It is known as sensitivity or true positive rate. It is metric quantifies ability of classification method to capture and properly detect each relevant instances of positive class.

$$\mathrm{Re}call = \frac{TP}{FN + TP} \tag{24}$$

5) Specificity

Specificity can be quit divers and can represent relationships in physics, chemistry, biology, economics, and many other disciplines. It is utilized to measure the ability of classification method to properly detect negative instances.

$$Specificity = \frac{TN}{TN + FP} \tag{25}$$

6) Error rate

It is used to scale degree of prediction error of method made with respect to true method. This is compared by the equation (26)

$$Errorrate = 100 - Accuracy \tag{26}$$

7) RoC

RoC is ratio of false negative to the true positive region, given in equation (27)

$$RoC = 0.5 \times \left(\frac{TP}{TP + FN} + \frac{TN}{TN + FP} \right) \tag{27}$$

B. Performance analysis

Figure 3 to 10 displays simulation results of AC-ASD-HSTCNN-GO technique. The AC-ASD-HSTCNN-GO is analysed to the existing GD-3DASDL-IST, GRADE-RR and ALN-RFA-NLAD respectively.

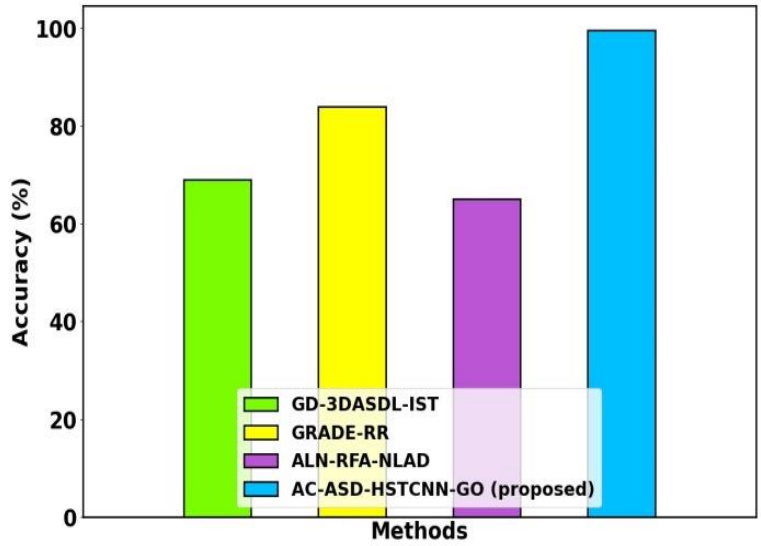

Figure 3: Accuracy analysis

Figure 3 displays accuracy analysis. The AC-ASD-HSTCNN technique attains 15.28%, 16.72%, 19.26% higher accuracy which analysed with existing GD-3DASDL-IST, GRADE-RR and ALN-RFA-NLAD methods respectively.

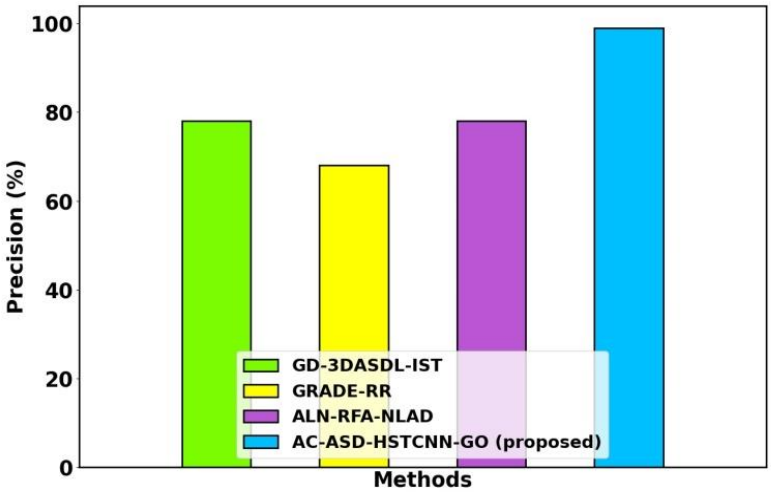

Figure 4: Precision analysis

Figure 4 displays precision analysis. The AC-ASD-HSTCNN-GO method attains 17.33%, 19.82%, 20.18% higher precision which analysed with existing GD-3DASDL-IST, GRADE-RR and ALN-RFA-NLAD methods respectively.

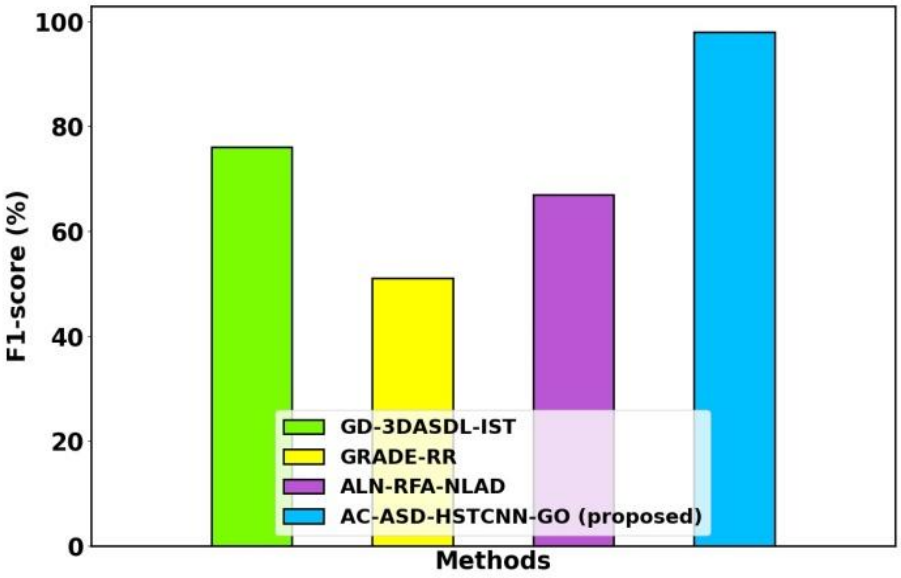

Figure 5: F1-score analysis

Figure 5 shows F1-score analysis. The AC-ASD-HSTCNN-GO method attains 18.35%, 20.92%, 21.39% higher F1-score which analysed with existing GD-3DASDL-IST, GRADE-RR and POTS-LSD-LPT methods respectively.

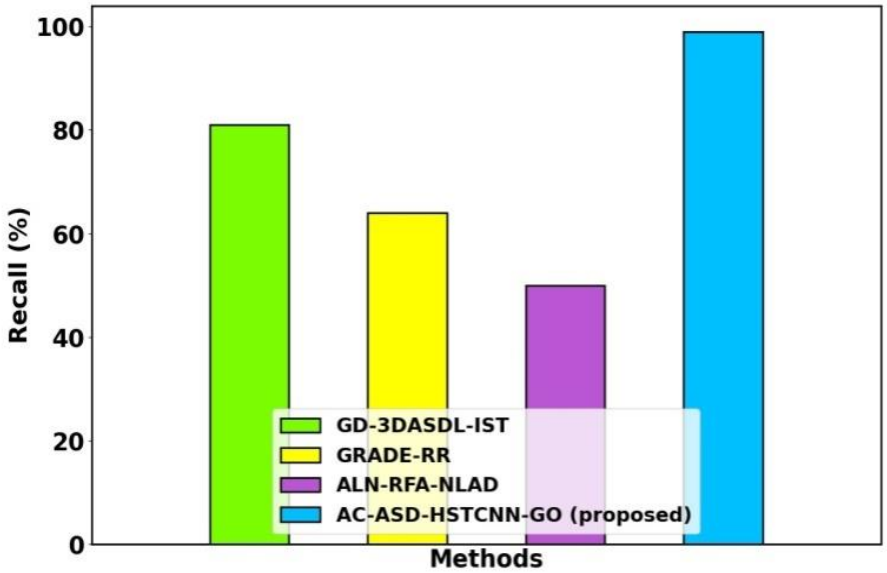

Figure 6: Recall analysis

Figure 6 displays recall analysis. The AC-ASD-HSTCNN-GO method attains 19.39%, 21.32%, 22.47% greater recall which analysed with existing GD-3DASDL-IST, GRADE-RR and ALN-RFA-NLAD methods respectively.

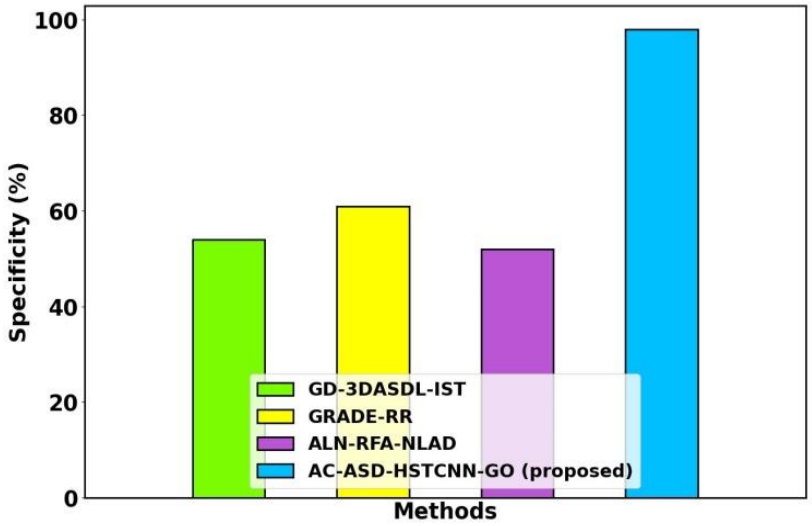

Figure 7: Specificity analysis

Figure 7 shows specificity analysis. The AC-ASD-HSTCNN-GO method attains 20.24%, 21.70%, 22.51% greater specificity which analysed with existing GD-3DASDL-IST, GRADE-RR and ALN-RFA-NLAD methods respectively.

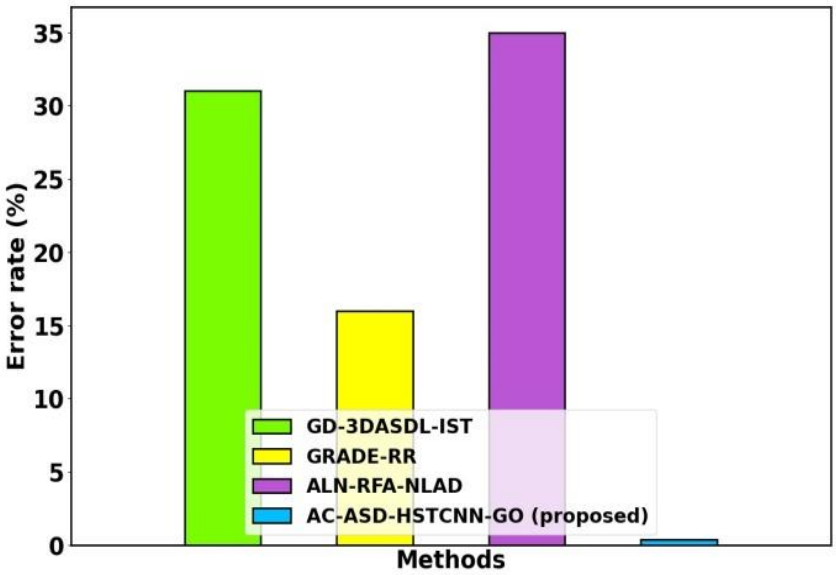

Figure 8: Error-rate analysis

Figure 8 displays error rate analysis. The proposed AC-ASD-HSTCNN-GO method attains 21.29%, 22.60%, 23.67% lower error rate which analysed with existing GD-3DASDL-IST, GRADE-RR and ALN-RFA-NLAD method respectively.

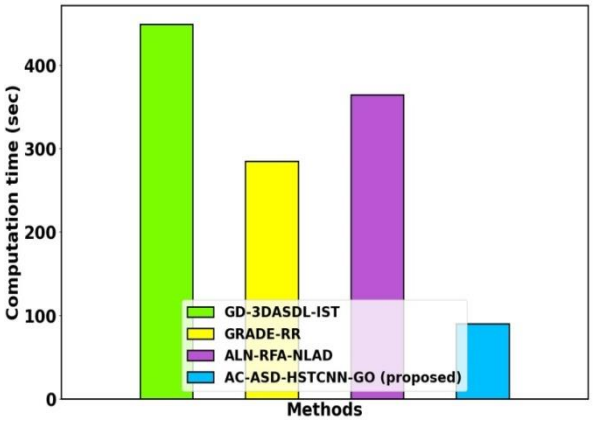

Figure 9: Computation time analysis

Figure 9 shows computation time analysis. The AC-AST-HSTCNN-GO technique attains 22.25%, 23.26%, and 24.74% lesser computation time analysed with existing techniques likes GD-3DASDL-IST, GRADE-RR and ALN-RFA-NLAD methods respectively.

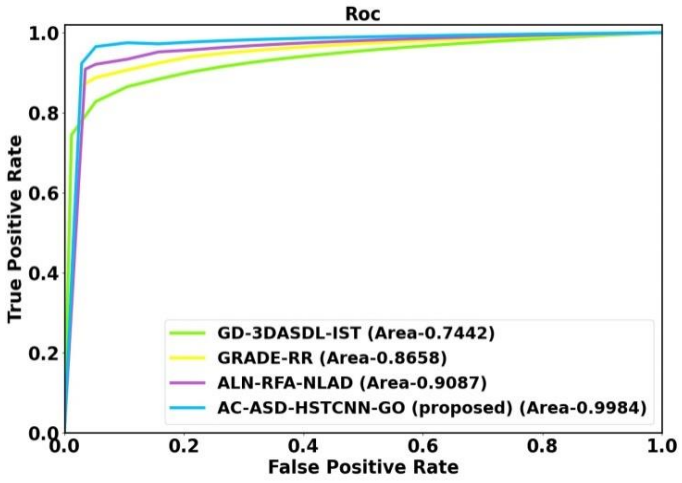

Figure 10: RoC analysis

Figure 10 shows RoC analysis. The AC-AST-HSTCNN-GOA method provides 23.82%, 24.61%, and 26.31% greater RoC analysed with existing techniques likes GD-3DASDL-IST, GRADE-RR and ALN-RFA-NLAD methods respectively.

C. Discussion

The use of the HSTGCNN method in 3D animation graphic design is examined in this research. By using better techniques, like stability of generator, discriminator is specifically enhanced to increase image quality. Even while the enhanced techniques have slightly increased training stability and result quality, they are still unable to completely address the challenges associated with HSTGCNN training, likes structure, gradient vanishing issues. They identified the difficulties in training DL models and enhanced U-Net method's accuracy in depth image estimate using novel loss function. This system demonstrated how AI may be used in end-use product design by autonomously generating 3D CAD drawings, assessing engineering performance. In conclusion, our work has increased the effectiveness and visual quality of 3D animation graphic design by using enhanced HSTGCNN method.

V. CONCLUSION

In this section, Artistic Creation and Animation Scene Designing using Hierarchical Spatio-temporal graph convolutional neural network Optimized with Gazelle Optimization Algorithm(AC-ASD-HSTCNN-GO) is successfully implemented in python.It is Utilizing a HSTCNN model raise the effectiveness of 3D animation visual design with precision method recognition.The performance of the proposed HSGCNN-SN-CPA methods provides 18.35%, 20.92%, 21.39% greater F1-Score 19.39%, 21.32%, 22.47% greater recall and 20.24%, 21.70%, 22.51% greater specificity when compared with existing methods such as GD-3DASDL-IST, IASD-AL-VR and LGFA-RSGAN-GNR respectively.

REFERENCE

[1] Xuan, D. (2023). Design of 3d animation color rendering system based on image enhancement algorithm and machine learning. *Soft Computing*, 1-10.

[2] Ji, B., Pan, Y., Yan, Y., Chen, R., & Yang, X. (2023). StyleVR: Stylizing Character Animations with Normalizing Flows. *IEEE Transactions on Visualization and Computer Graphics.*

[3] Kalmakurki, M. (2022). Digital character costume design in computer-animated feature films. *Näyttämö ja tutkimus*, *9*, 243-246.

[4] Wang, Y., Zhang, N., Chen, D., & Vongphantuset, J. (2022). Animation design using virtual reality modelling and fractal morphing technology. *Fractals*, *30*(02), 2240100.

[5] Sutrisno, A. (2022). Designing Animated Infographics about Thesis Defence Registration Procedures. *KnE Social Sciences*, 147-156.

[6] Hidayat, M.T., Rahim, S.S., Parumo, S., A'bas, N.N., Sani, M.A.M., & Aziz, H.A. (2022). Designing a Two-Dimensional Animation for Verbal Apraxia Therapy for Children with Verbal Apraxia of Speech. *Ingénierie des Systèmes d'Information*, *27*(4).

[7] Tang, T., Li, P., & Tang, Q. (2022). New strategies and practices of design education under the background of artificial intelligence technology: online animation design studio. *Frontiers in Psychology*, *13*, 767295.

[8] Li, S. (2023). Application of artificial intelligence-based style transfer algorithm in animation special effects design. *Open Computer Science*, *13*(1), 20220255.

[9] Wang, D., & Lee, J. (2022). Convolution-Based Design for Real-Time Pose Recognition and Character Animation Generation. *Wireless Communications and Mobile Computing*, *2022.*

[10] Peng, Y., Zhao, C., Xie, H., Fukusato, T., Miyata, K., & Igarashi, T. (2023). DualMotion: Global-to-Local Casual Motion Design for Character Animations. *IEICE TRANSACTIONS on Information and Systems*, *106*(4), 459-468.

[11] Rao, N., Perdomo, S., & Jonassaint, C. (2022). A novel method for digital pain assessment using abstract animations: human-centered design approach. *JMIR Human Factors*, *9*(1), e27689.

[12] Parmar, D., Olafsson, S., Utami, D., Murali, P., & Bickmore, T. (2022). Designing empathic virtual agents: manipulating animation, voice, rendering, and empathy to create persuasive agents. *Autonomous agents and multi-agent systems*, 36(1), 17.

[13] Zong, J., Pollock, J., Wootton, D., & Satyanarayan, A. (2022). Animated Vega-Lite: A Unified Grammar of Interactive and Animated Visualizations. *arXiv preprint arXiv:*2208.03869.

[14] Li, L., & Li, T. (2022). Animation of virtual medical system under the background of virtual reality technology. *Computational Intelligence*, *38*(1), 88-105.

[15] Xing, J., Xia, M., Zhang, Y., Chen, H., Wang, X., Wong, T.T., & Shan, Y. (2023). Dynamic rafter: Animating open-domain images with video diffusion priors. *ArXiv preprint arXiv*: 2310.12190.

[16] Mukundan, R. (2022). 3D Mesh Processing and Character Animation: With Examples Using OpenGL, OpenMesh and Assimp. *Springer Nature*.

[17] Eid, M.G. (2022). Benefits of animated advertisements in today's world (Doctoral dissertation, Notre Dame University-Louaize).

[18] Tan, S. (2022). Animation Image Art Design Mode Using 3D Modeling Technology. *Wireless Communications and Mobile Computing, 2022*.

[19] Zeng, B., Liu, B., Li, H., Liu, X., Liu, J., Chen, D., Peng, W., & Zhang, B. (2022). FNeVR: Neural volume rendering for face animation. *Advances in Neural Information Processing Systems*, *35*, 22451-22462.

[20] Li, Y., & Zhuge, W. (2022). Application of Animation Control Technology Based on Internet Technology in Digital Media Art. *Mobile Information Systems*, *2022*.

[21] Tang, J. (2023). Graphic Design of 3D Animation Scenes Based on Deep Learning and Information Security Technology. *Journal of ICT Standardization*, *11*(3), 307-328.

[22] Bonetto, E., Xu, C., & Ahmad, A. (2023). GRADE: Generating realistic animated dynamic environments for robotics research. *ArXiv preprint arXiv:* 2303.04466.

[23] Zhao, L., & Zhang, K. (2022). Application of a Random Forest Algorithm in Natural Landscape Animation Design. *Computational Intelligence and Neuroscience*, *2022.*

[24] Shan, F., & Wang, Y. (2022). Animation design based on 3D visual communication technology. *Scientific Programming, 2022*, 1-11.

[25] Li, X., Zhang, C., & Wu, Y. (20220. Deconstruction of Immersive Animation Image Interaction Design under Virtual Reality Technology. *Wireless Communications and Mobile Computing, 2022*.

[26] Wu, H., Wen, S.J., & Yang, J.H. (2022). Multimedia Character Modeling Design and Modeling of Cartoon Animation Based on Bayesian Sequence Recommendation Algorithm. *Computational Intelligence and Neuroscience, 2022*.

[27] Xu, J., Liu, K., & Yuan, Y. (2022). A novel MG 2D animation design method under the perspective of convergence media using intelligent design technology.*Computational Intelligence and Neuroscience, 2022*.

[28] https://www.kaggle.com/datasets/karimcossentini/velodyne-point-cloud-dataset

[29] Ge, Y., Yang, L., & Ma, X. (2021). A harmonic compensation method for SPMSM sensorless control based on the orthogonal master-slave adaptive notch filter. *IEEE Transactions on Power Electronics*, *36*(10), 11701-11711.

[30] Meng, Z., Lv, M., Liu, Z., & Fan, F. (2021). General Synchroextracting Chirplet transform: Application to the rotor rub-impact fault diagnosis. *Measurement*, *169*, 108523.

[31] Zeng, X., Jiang, Y., Ding, W., Li, H., Hao, Y., & Qiu, Z. (2021). A hierarchical spatio-temporal graph convolutional neural network for anomaly detection in videos. *IEEE Transactions on Circuits and Systems for Video Technology*.

[32] Agushaka, J.O., Ezugwu, A.E., & Abualigah, L. (2023). Gazelle optimization algorithm: a novel nature-inspired metaheuristic optimizer. *Neural Computing and Applications, 35(*5), 4099-4131.